Wireless Personal Communications **21:** 29–48, 2002.

Closed-Form Estimators for Blind Separation of Sources – Part II: Complex Mixtures

VICENTE ZARZOSO* and ASOKE K. NANDI
Signal Processing and Communications Group, Department of Electrical Engineering and Electronics, The University of Liverpool, Brownlow Hill, Liverpool L69 3GJ, U.K.
E-mail: vicente@liverpool.ac.uk

Abstract. The problem of multiuser detection in wireless communications systems adopts, in flat-fading channels, a blind source separation (BSS) formulation of instantaneous linear mixtures. This contribution addresses the closed-form solutions to BSS in the complex-mixture scenario. The algebraic devices which span a unifying framework for the complex BSS closed-form estimators are developed. With the aid of these tools, results originally encountered in the real-mixture case are extended to the complex case, thus highlighting the remarkable parallelism existing between the real and complex problems in the context of their analytic solutions. Computer simulations illustrate the theoretical results and compare the proposed methods to other BSS procedures.

Keywords: bicomplex numbers, blind source separation, closed-form estimators, complex mixtures, higher-order statistics, independent component analysis, multiuser detection.

1. Introduction

1.1. Problem Statement

CDMA's many attractive features ("soft capacity", "soft handover", inherently dynamic channel sharing, etc.) have transformed it into the preferred multiple access technique for third generation wireless personal communications [20]. Since the quality of CDMA systems degrades with the interference caused by users operating in the same cell, active suppression of multiuser interference (MUI) leads to considerable performance gains. Multiuser detection (MUD) [26, 27] techniques take advantage of the particular structure of MUI in order to extract the signal(s) of interest free from interference. This process implicitly involves the recovery of the users' transmitted signals that are mixed at the receiving antenna. In flat-fading environments [21], the signals observed at a sensor array output $\boldsymbol{y} = [y_1, \ldots, y_p]^{\mathrm{T}} \in \mathbb{C}^p$ can be considered as unknown instantaneous mixtures of the transmitted data signals $\boldsymbol{x} = [x_1, \ldots, x_q]^{\mathrm{T}} \in \mathbb{C}^q$:

$$\boldsymbol{y} = \boldsymbol{M}\boldsymbol{x} \,. \tag{1}$$

The unknown mixing matrix $\boldsymbol{M} \in \mathbb{C}^{p\times q}$ is determined by the spreading waveforms, propagation conditions, source-sensor positions, etc. Hence, MUD reduces to the estimation of users' data $\boldsymbol{x}$ from the observations $\boldsymbol{y}$, a problem which corresponds the blind source separation (BSS) of instantaneous linear mixtrues [31]. A myriad of other applications, in areas as diverse

* Supported through a Post-doctoral Research Fellowship awarded by the Royal Academy of Engineering, U.K.

as biomedical signal processing [15, 16, 22], seismic exploration [14, 24], radar and sonar, speech processing [25], etc., can also be modelled from the perspective of BSS. Due to this wide range of applications, the BSS problem has aroused great research interest over the last decade.

Only two assumptions usually suffice to achieve the separation, namely, that the source signals be statistically independent and the matrix $\boldsymbol{M}$ be full column rank. Even counting on these fundamental hypotheses, the solution to the BSS problem suffers from inherent indeterminacies related to the order and the scale of the recovered sources. Both are unimportant in most practical situations. As a consequence, it can be assumed without loss of generality that the sources are unit-variance.

The convenience of tackling the problem in two steps has been endorsed in a great number of works [4, 6–10, 12–14, 19, 30, 31]. The first step, known as pre-whitening, involves second-order statistics (SOS) and yields a set of uncorrelated normalized signals, so-called whitened observations. The second step accomplishes the source separation and mixing matrix identification by means of the higher-order statistics (HOS) of the data. The justification for the first SOS-based step is twofold: (a) since SOS are generally estimated with higher accuracy than HOS, it seems sensible to benefit from the former before resorting to the latter, and (b) after pre-whitening, the dimensionality of the problem is reduced. Effectively, the whitened observations $\boldsymbol{z}$ are related to the true sources through a unitary transformation $\boldsymbol{Q} \in \mathbb{C}^{q \times q}$:

$$\boldsymbol{z} = \boldsymbol{Q}\boldsymbol{x} \,, \tag{2}$$

from where it becomes apparent that fewer parameters remain to be estimated relative to the initial model (1).

1.2. Closed-Form Solutions

Several different approaches exist to cope with the BSS problem [4, 8, 31], but we are primarily concerned with the closed-form or analytical solutions which yield direct estimators for the mixing-structure elements. In the two-source two-sensor scenario, direct solutions are found for model (1) without the need for a pre-whitening stage [5, 17]. However, this is at the expense of constraining the mixing matrix structure, resulting in the loss of the uniform performance property [3, Section III-E]. The desirable uniform performance feature means that the separation quality depends only on the source distribution, but not on the particular mixing structure [2, 3].

For this reason, our focus is rather on the direct estimation of matrix $\boldsymbol{Q}$ after pre-whitening, where no such constraints on the mixing structure are made. In [6] the first analytical expression (*Comon's formula, CF*) was proposed for the real-mixture case, based on the 4th-order cumulants. The extension of this idea to the complex-signal environment (*complex CF*, CCF) was carried out in [7], [9] and [13]. Also for the real-mixture scenario, the maximum-likelihood (ML) approach was adopted in [12], and with the help of Gram–Charlier expansion of the source probability density function (pdf), another closed-form estimator (*approximate ML, AML*) was obtained for symmetric sources with identical distribution and positive kurtosis. Those restrictions were spared with the estimator developed in [30] (*extended ML, EML*). Another of such expressions (*sum of output kurtosis, SOK*) was found in [10] as the closed-form solution to the maximimization of a contrast function proposed in [19]. The connection among the above estimators for the real case was accomplished in [33]. The relationship between the CF, the AML and the EML was unveiled and the performance of the CF analyzed.

A family of closed-form estimators based on the nth-order cumulants was developed, of which the EML was found to be a particular case (at order $n = 4$). The family was associated with the respective cost function optimization criteria, which led to the link between the EML and the SOK solutions. Also, a novel 4th-order estimator (*alternative EML, AEML*) was proposed, in conjunction with an empirically-derived decision rule, in order to overcome a deterioration in performance of the other 4th-order estimators for null source kurtosis sum (sks).

1.3. Objectives and Organization

In MUD, as well as in other communications problems, digital modulations and channel effects are conveniently described via complex-valued (phasor) representations, which result in a BSS model of complex mixtures. Solving the complex-mixture problem is also of interest in other important applications such as seismic sounding [14, 24]. The purpose of this paper is to extend to the complex case some of the results unfolded in [33] for the real-mixture scenario. In particular, we want to lay emphasis on the existing analogy between the direct solutions to the real and complex problems. The definition of a special set of numbers in accordance with the particular structure of matrix $\boldsymbol{Q}$ plays a crucial role in achieving these objectives.

The contents are divided in the following sections. In the first place, Section 2 deals with the peculiarities of the problem in the complex case, and sets the statistical nomenclature that will be used for complex variables. Section 3 defines a new number class – so called *bicomplex numbers* – in compliance with the structure and properties of the unitary transformation to be identified. By using this new tool, a family of closed-form estimators based on the HOS (the higher-order cumulants) of the whitened signals is disclosed in Section 4. This family is totally analogous to the one found for the real case in [33]. At fourth order, the general expression reduces to the complex extension of the EML estimator of [30]. Similarly as occurred for its real counterpart, this 4th-order estimator suffers a performance degradation when the sks is near zero. To surmount this limitation, a hybrid estimation procedure is proposed, featuring an alternative estimator also based on 4th-order cumulants. The simulations reported in Section 6 illustrate these results and compare the methods studied to other BSS techniques. Conclusions are left for Section 7. Table 1 lists all the acronyms employed throughout the paper.

2. Complex Mixtures

2.1. Problem Paraterization and Equivalence Class of Valid Solutions

In the complex case, the 2×2 unitary transformation $\boldsymbol{Q}$ becomes a unitary matrix, with the generic shape:

$$\boldsymbol{Q} = \begin{bmatrix} a & -b^* \\ b & a^* \end{bmatrix}, \tag{3}$$

symbol * representing complex conjugation. Up to (irrelevant, due to the source scaling indeterminacy) pre-multiplication by a unit-norm diagonal matrix, the above matrix reduces to a complex Givens rotation, which exhibits the general form:

$$\boldsymbol{Q} = \boldsymbol{\mathcal{Q}}(\theta, \alpha), \tag{4}$$

with

$$\boldsymbol{\mathcal{Q}}(\cdot,\cdot) : \mathbb{R} \times \mathbb{R} \mapsto \mathbb{C}^{2\times 2}, \qquad \boldsymbol{\mathcal{Q}}(\theta,\alpha) = \begin{bmatrix} \cos\theta & -\mathrm{e}^{-j\alpha}\sin\theta \\ \mathrm{e}^{j\alpha}\sin\theta & \cos\theta \end{bmatrix}. \tag{5}$$

Table 1. List of acronyms.

Acronym	Definition
AEML	alternative EML
AML	approximate maximum likelihood
BSS	blind source separation
CAEML	complex AEML
CCF	complex CF
CDMA	code division multiple access
CEML	complex EML
CF	Comon's formula
combCCF	combined CCF
combCEML	combined CEML
EML	extended maximum likelihood
HOS	higher-order statistics
ISR	interference-to-signal ratio
JADE	joint approximate diagonalization of eigenmatrices
MC	Monte Carlo
ML	maximum likelihood
MUD	multiuser detection
MUI	multiuser interference
pdf	probability density function
PRBS	pseudorandom binary sequence
QAM	quadrature amplitude modulation
skd	source kurtosis difference
sks	source kurtosis sum
SNR	signal-to-noise ratio
SOK	sum of output kurtosis
SOS	second-order statistics
SVD	singular value decomposition

Therefore, two parameters, angle θ and phase α, need to be estimated in order to achieve the identification of the relevant matrix, and hence the source extraction. If $\hat{\theta}$ and $\hat{\alpha}$ represent estimates of θ and α, respectively, then the source separation is attained through

$$\hat{\boldsymbol{x}} = \widehat{\boldsymbol{Q}}^{\mathrm{H}} \boldsymbol{z} = \widehat{\boldsymbol{Q}}^{\mathrm{H}} \boldsymbol{Q} \boldsymbol{x}, \qquad \widehat{\boldsymbol{Q}} = \boldsymbol{\mathcal{Q}}(\hat{\theta}, \hat{\alpha}) \,. \tag{6}$$

The actual values of (θ, α) are not the only solutions to provide a valid source extraction. Due to the indeterminacies commented in Section 1.1, any solution of the form

$$\boldsymbol{G} \triangleq \widehat{\boldsymbol{Q}}^{\mathrm{H}} \boldsymbol{Q} = \boldsymbol{P} \boldsymbol{D} \,, \tag{7}$$

with $\boldsymbol{P}$ a permutation and $\boldsymbol{D}$ a regular diagonal matrix is considered as acceptable, since it preserves the source waveforms. Accordingly, the following set of solutions are equivalent in the waveform-preserving sense to (θ, α), i.e., $(\hat{\theta}, \hat{\alpha}) \equiv (\theta, \alpha)$:

$$(\hat{\theta}, \hat{\alpha}) = \left(\theta + \frac{m\pi}{2}, \alpha + 2\pi n\right), \quad \text{and} \tag{8a}$$

$$(\hat{\theta}, \hat{\alpha}) = \left(-\theta + \frac{m\pi}{2}, \alpha + (2n+1)\pi\right), \quad n, m \in \mathbb{N}. \tag{8b}$$

Hence, we call $[(\theta, \alpha)] \triangleq \{(\hat{\theta}, \hat{\alpha}) \in \mathbb{R}^2 \mid (\hat{\theta}, \hat{\alpha}) \equiv (\theta, \alpha)\}$ the *equivalence class of valid solutions* of our problem.

2.2. Complex-Variate Statistics

The methods studied in this paper rely on the higher-order cumulants of the data. There are different possible natural ways to define the cumulants for complex variables [1]. For our purposes, however, it is convenient to choose:

$$\mathrm{Cum}^z_{i_1 i_2 i_3 \ldots} \triangleq \mathrm{Cum}[z^*_{i_1}, z_{i_2}, z^*_{i_3}, \ldots]. \tag{9}$$

The same pairwise conventions as those defined in [33] hold (Kendall's convention [23]):

$$\kappa^z_{n-r,r} \triangleq \mathrm{Cum}^z_{\underbrace{1\ldots1}_{n-r}\underbrace{2\ldots2}_{r}}. \tag{10}$$

For unit-variance zero-mean uncorrelated components, the expressions for the 4th-order cumulants are:

$$\begin{aligned}
&\kappa^z_{40} = \mathrm{E}[|z_1|^4] - |\mathrm{E}[z_1^2]|^2 - 2, \quad \kappa^z_{31} = \mathrm{E}[z_1^*|z_1|^2 z_2] \\
&\kappa^z_{22} = \mathrm{E}[|z_1|^2|z_2|^2] - 1, \quad \kappa^z_{13} = \mathrm{E}[z_1^*|z_2|^2 z_2] \\
&\kappa^z_{04} = \mathrm{E}[|z_2|^4] - |\mathrm{E}[z_2^2]|^2 - 2,
\end{aligned} \tag{11}$$

where $\mathrm{E}[\cdot]$ denotes the mathematical expectation. Note that certain cumulants may take complex values (such as κ^z_{31} and κ^z_{13} above). It is precisely from these complex-valued cumulants that the complex phase α can be estimated.

Owing to the linear relationship between the whitened observations and the source signals represented by Equations (2), (4) and (5), and the multilinearity property of cumulants [18, Section 2.4], we have:

$$\begin{aligned}
\kappa^z_{40} &= \cos^4\theta\kappa^x_{40} + \sin^4\theta\kappa^x_{04} \\
\kappa^z_{31} &= \cos^3\theta\sin\theta\mathrm{e}^{j\alpha}\kappa^x_{40} - \sin^3\theta\cos\theta\mathrm{e}^{j\alpha}\kappa^x_{04} \\
\kappa^z_{22} &= \cos^2\theta\sin^2\theta(\kappa^x_{40} + \kappa^x_{04}) \\
\kappa^z_{13} &= \cos\theta\sin^3\theta\mathrm{e}^{j\alpha}\kappa^x_{40} - \sin\theta\cos^3\theta\mathrm{e}^{j\alpha}\kappa^x_{04} \\
\kappa^z_{04} &= \sin^4\theta\kappa^x_{40} + \cos^4\theta\kappa^x_{04}.
\end{aligned} \tag{12}$$

3. Bicomplex Numbers

The use of complex numbers facilitates the closed-form identification of the orthogonal mixing matrix in the real case [30, 33]. Since we are now dealing with complex mixtures, it seems

natural to seek certain type of extension of the complex numbers. We carry out such extension as follows.

DEFINITION 1 (bicomplex number). *A* bicomplex number $\bar{x} \in \mathbb{B}$ *is an expression of the form:*

$$\bar{x} = a + \jmath\jmath b, \quad a, b \in \mathbb{C}, \jmath\jmath^2 = -1\,. \tag{13}$$

Although symbol $\jmath\jmath$ has the same numeric value as the usual imaginary unit $\jmath$, it must be understood as "orthogonal" to or in a "different space" from that of $\jmath$, so that they actually repesent distinct algebraic elements.

DEFINITION 2 (breal and bimaginary part). *Given* $\bar{x} = a + \jmath\jmath b \in \mathbb{B}, \mathbb{R}\mathrm{e}(\bar{x}) = a \in \mathbb{C}$ *is the* bicomplex-real (breal) *part of* $\bar{x}$*, and* $\mathbb{I}\mathrm{m}(\bar{x}) = b \in \mathbb{C}$ *its* bicomplex-imaginary (bimaginary) *part.*

This terminology prevents confusion with the commonplace real [Re(·)] and imaginary [Im(·)] parts of complex numbers, which are always real valued. Accordingly, $\jmath\jmath$ is named *bimaginary unit*. Due to the nature of the matrix to be identified, our attention is restricted to the subset:

DEFINITION 3 (unitary bicomplex number). $\mathbb{B}_u = \{\bar{x} \in \mathbb{B} : |a|^2 + |b|^2 = 1\}$ *is the set of* unitary *bicomplex numbers.*

It is straightforward to establish an isomorphism between the set of bicomplex numbers and a particular set of matrices related to our problem. Let us first define this matrix set.

DEFINITION 4. $\mathcal{U}$ *is the set of* unitary 2×2 *matrices:* $\mathcal{U} = \{\boldsymbol{U} \in \mathbb{C}^{2\times 2} : \boldsymbol{U}\boldsymbol{U}^{\mathrm{H}} = \boldsymbol{U}^{\mathrm{H}}\boldsymbol{U} = I\}$.

The set $\mathcal{U}$ under ordinary matrix multiplication forms a non-Abelian group. In particular, $\mathcal{U}$ is a subgroup of SL(2, $\mathbb{C}$), the so-called special linear group of 2×2 matrices over $\mathbb{C}$ [11]. Any matrix $\boldsymbol{U} \in \mathcal{U}$ can be written in general form as:

$$\boldsymbol{U} = \begin{bmatrix} a & -b^* \\ b & a^* \end{bmatrix}, \quad a, b \in \mathbb{C}, \quad |a|^2 + |b|^2 = 1\,. \tag{14}$$

The product of two unitary matrices is given by:

$$\boldsymbol{U}_1\boldsymbol{U}_2 = \begin{bmatrix} a_1a_2 - b_1^*b_2 & -a_1b_2^* - b_1^*a_2^* \\ b_1a_2 + a_1^*b_2 & -b_1b_2^* + a_1^*a_2^* \end{bmatrix}. \tag{15}$$

Now, we can define the *product* of two bicomplex numbers $\bar{x}_1$ and $\bar{x}_2$ in compliance with the product of $\mathcal{U}$-matrices by regarding the first column of the previous expression, so that:

$$\bar{x}_1\bar{x}_2 \triangleq [\mathbb{R}\mathrm{e}(\bar{x}_1)\mathbb{R}\mathrm{e}(\bar{x}_2) - \mathbb{I}\mathrm{m}^*(\bar{x}_1)\mathbb{I}\mathrm{m}(\bar{x}_2)] + \jmath\jmath[\mathbb{I}\mathrm{m}(\bar{x}_1)\mathbb{R}\mathrm{e}(\bar{x}_2) + \mathbb{R}\mathrm{e}^*(\bar{x}_1)\mathbb{I}\mathrm{m}(\bar{x}_2)]\,. \tag{16}$$

With this product operation: $\jmath\jmath^2 = -1$, in agreement with Definition 1. Also, if both the breal and bimaginary parts of the bicomplex operands are real, such product reduces (changing $\jmath$ for $\jmath\jmath$) to the usual complex-number multiplication. Hence, Equation (16) is a natural generalization of the complex product. By virtue of these conventions, the mapping

$$\aleph : \mathcal{U} \mapsto \mathbb{B}_u\,, \tag{17}$$

with

$$\aleph(\boldsymbol{U}) = u_{11} + \jmath u_{21} = a + \jmath b, \quad \boldsymbol{U} \in \mathcal{U}\,, \tag{18}$$

represents an isomorphism between $\mathcal{U}$ under normal matrix multiplication and $\mathbb{B}_u$ under the bicomplex-number product as defined in (16). Effectively, $\aleph(\cdot)$ is one-to-one, onto and operation preserving, conditions that must be fulfilled by any isomorphism [11]. From the former two conditions, any $\bar{x} = a + \jmath b \in \mathbb{B}_u$ can be uniquely associated to the first column of one and only one matrix $\boldsymbol{U} = [\boldsymbol{u}_1, \boldsymbol{u}_2] = \aleph^{-1}(\bar{x}) \in \mathcal{U}$, $\boldsymbol{u}_1 = [a, b]^{\mathrm{T}}$. The latter condition is due to (16), which guarantees $\aleph(\boldsymbol{U}_1\boldsymbol{U}_2) = \aleph(\boldsymbol{U}_1)\aleph(\boldsymbol{U}_2)$. Therefore, the related sets are isomorphic: $\mathcal{U} \sim \mathbb{B}_u$. Having established this connection, and owing to the properties of isomorphisms, the following definitions naturally follow, $\forall \bar{x} \in \mathbb{B}$:

DEFINITION 5 (conjugation). $\bar{x}^* = \mathbb{R}\mathrm{e}(\bar{x})^* - \jmath\,\mathbb{I}\mathrm{m}(\bar{x})$.

This is because the first column of $\boldsymbol{U}^{\mathrm{H}}$ is $[a^*, -b]^{\mathrm{T}}$.

DEFINITION 6 (modulus). $|\bar{x}|^2 = \bar{x}\bar{x}^* = \bar{x}^*\bar{x} = |\mathbb{R}\mathrm{e}(\bar{x})|^2 + |\mathbb{I}\mathrm{m}(\bar{x})|^2$.

Effectively, the first column of $\boldsymbol{U}\boldsymbol{U}^{\mathrm{H}}$ and $\boldsymbol{U}^{\mathrm{H}}\boldsymbol{U}$ is given by $[|a|^2+|b|^2, 0]^{\mathrm{T}}$. As an immediate consequence:

DEFINITION 7 (inverse). $\bar{x}^{-1} = \bar{x}^*/|\bar{x}|^2$.

For instance, $\jmath^{-1} = -\jmath$, just like its complex twin j.

If the unitary transformation is parameterized like in (4)–(5), then the associated unitary bicomplex number becomes an important particular case.

DEFINITION 8 (bicomplex exponential). *Expression*

$$\mathrm{e}_\alpha^{\jmath\theta} \triangleq \cos\theta + \jmath \mathrm{e}^{j\alpha} \sin\theta, \quad \theta, \alpha \in \mathbb{R}\,, \tag{19}$$

is called bicomplex exponential*, by analogy with its familiar complex counterpart.*

The following properties of the bicomplex exponential are easily proven, $\forall n \in \mathbb{N}$, $\forall \theta, \theta_1$, $\theta_2, \alpha \in \mathbb{R}$:

$$\text{(i)}\ \ \mathrm{e}_\alpha^{\jmath\theta_1}\mathrm{e}_\alpha^{\jmath\theta_2} = \mathrm{e}_\alpha^{\jmath\theta_2}\mathrm{e}_\alpha^{\jmath\theta_1} = \mathrm{e}_\alpha^{\jmath(\theta_1+\theta_2)},\ \text{and hence}\ (\mathrm{e}_\alpha^{\jmath\theta})^n = \mathrm{e}_\alpha^{\jmath n\theta} \tag{20a}$$

$$\text{(ii)}\ \ (\mathrm{e}_\alpha^{\jmath\theta})^{-1} = (\mathrm{e}_\alpha^{\jmath\theta})^* = \mathrm{e}_\alpha^{-\jmath\theta} \tag{20b}$$

$$\text{(iii)}\ \ \mathrm{e}_{\alpha\pm\pi}^{\jmath\theta} = \mathrm{e}_\alpha^{-\jmath\theta} \tag{20c}$$

$$\text{(v)}\ \ \mathrm{e}_\alpha^{\jmath(\theta+\frac{n\pi}{2})} = \begin{cases} (-1)^{\frac{n}{2}}\mathrm{e}_\alpha^{\jmath\theta}, & n \text{ even} \\ (-1)^{\frac{n-1}{2}}\jmath\,\mathrm{e}^{j\alpha}\mathrm{e}_\alpha^{\jmath\theta}, & n \text{ odd.} \end{cases} \tag{20d}$$

The bimaginary unit can be written as $\jmath = \mathrm{e}_0^{\jmath\frac{\pi}{2}}$, so that, as an important special case of (20d):

$$\text{(vi)}\ \ \jmath^n = \begin{cases} (-1)^{\frac{n}{2}}, & n \text{ even} \\ (-1)^{\frac{n-1}{2}}\jmath, & n \text{ odd,} \end{cases} \tag{20e}$$

identities which again highlight the similarity between the bimaginary and the imaginary units. Another immediate consequence of property (20d) is that $\mathrm{e}_{\alpha}^{\jmath\jmath\frac{n\pi}{2}}$ is always a pure breal (n even) or pure bimaginary (n odd) bicomplex quantity, which correspond to unitary matrices of the form $\boldsymbol{P}\boldsymbol{D}$ [Equation (7)]. Hence, global matrix $\boldsymbol{G}$ represents a valid separating solution if and only if its associated bicomplex number $\aleph(\boldsymbol{G})$ is pure breal or pure bimaginary. As $\boldsymbol{G} = \widehat{\boldsymbol{Q}}^{\mathrm{H}}\boldsymbol{Q}$, then $\aleph(\boldsymbol{G}) = \aleph(\widehat{\boldsymbol{Q}})^{*}\aleph(\boldsymbol{Q}) = (\mathrm{e}_{\hat{\alpha}}^{\jmath\jmath\hat{\theta}})^{*}e_{\alpha}^{\jmath\jmath\theta}$. Now, straightforward application of properties (20) lead to the equivalent class of valid solutions (8), thus efficiently formulated in the bicomplex domain.

The next definition extends the argument ("arg") function.

DEFINITION 9 (barg function). *Given* $\bar{x} = |\bar{x}|\mathrm{e}_{\alpha}^{\jmath\jmath\theta}$, *let the* bicomplex argument (barg) *function be defined as*

$$(\psi, \varphi) = \measuredangle\bar{x}, \qquad \begin{cases} \psi = \angle(\mathbb{R}\mathrm{e}(\bar{x}) + j|\mathbb{I}\mathrm{m}(\bar{x})|) \\ \varphi = \angle\mathbb{I}\mathrm{m}(\bar{x}), \end{cases} \tag{21}$$

where $\angle(\cdot) \in]-\pi, \pi]$ *provides the angle with respect the real axis of its complex argument. Then:* $\mathrm{e}_{\varphi}^{\jmath\jmath\psi} = \mathrm{e}_{\alpha}^{\jmath\jmath\theta}$. *In particular:* $(\psi, \varphi) \equiv (\theta, \alpha)$.

In the real-mixture case, the so-called *scatter diagram* allows to simplify the development and provides an insightful geometrical interpretation of the real rotation taking place over the source signals after pre-whitening [12, 30, 31]. If $\boldsymbol{z} = \boldsymbol{\mathcal{Q}}(\theta)\boldsymbol{x}$, with $\boldsymbol{\mathcal{Q}}(\theta) = \boldsymbol{\mathcal{Q}}(\theta, 0)$ and $\boldsymbol{x}, \boldsymbol{z} \in \mathbb{R}^2$, then $z_1 + jz_2 = \mathrm{e}^{j\theta}(x_1 + jx_2)$. Taking into account bicomplex multiplication rule (16) and exponential expression (19), it is straightforward to prove that a similar relationship holds in the complex-mixture case too.

PROPOSITION 10 (bicomplex scatter-diagram). *If* $\boldsymbol{z} = \boldsymbol{\mathcal{Q}}(\theta, \alpha)\boldsymbol{x}$ *then*

$$\bar{z} = \mathrm{e}_{\alpha}^{\jmath\jmath\theta}\bar{x}\,, \tag{22}$$

with $\bar{x} = (x_1 + \jmath\jmath x_2)$ *and* $\bar{z} = (z_1 + \jmath\jmath z_2)$. *By analogy to the real case, the bicomplex numbers* $\bar{x}$ *and* $\bar{z}$ *are called* bicomplex scatter-diagram *points of the source and whitened signals, respectively.*

In the real case, the remaining orthogonal transformation after pre-whitening is easily interpreted as a geometric rotation of the scatter plots. By contrast, in the complex case both the scatter-diagram points and the associated "rotation" defined above, though algebraically analogous to its real-mixture equivalent, become less illuminating as a geometric notion.

Many of the above new concepts will allow us to simplify the notation of the complex-case closed-form estimators which are presented next. The beauty of bicomplex numbers is that by constraining the breal and bimaginary parts to be real quantities, i.e., the associated transformation to have real elements, one is at once dealing with the familiar complex numbers and, in the context of BSS, with the real-mixture scenario.

4. Complex Analytic Estimators

With the aid of the bicomplex-number tools developed in the previous section, [33, Theorem 1] accepts the following extension to complex mixtures, which is proved in the Appendix.

THEOREM 11. *Define $\bar{\xi}_n(\boldsymbol{z})$ as the following bicomplex weighted sum of pairwise nth-order cumulants of the components of $\boldsymbol{z}$, with $n \in \mathbb{N}^+$:*

$$\bar{\xi}_n(\boldsymbol{z}) \triangleq \sum_{r=0}^{n} \binom{n}{r} \jmath\jmath^r \kappa^{z}_{n-r,r} \,. \tag{23}$$

If $\boldsymbol{z} = \boldsymbol{\mathcal{Q}}(\theta, \alpha)\boldsymbol{x}$, with $\boldsymbol{x}$ made up of independent components, then:

$$\bar{\xi}_n(\boldsymbol{z}) = \mathrm{e}^{\jmath\jmath n\theta}_{(-1)^n\alpha} \bar{\xi}_n(\boldsymbol{x}) \,, \tag{24}$$

where, according to (23),

$$\bar{\xi}_n(\boldsymbol{x}) = \kappa^{x}_{n0} + \jmath\jmath^n \kappa^{x}_{0n} \,. \tag{25}$$

By analogy with the real case, cumulant combination (23) is termed whitened-observation *nth-order bicomplex centroid*. If $\xi_n(\boldsymbol{x})$ is known or can be estimated, parameters (θ, α) may be readily obtained in closed-form from (24) via:

$$(n\hat{\theta}, \hat{\alpha}) = \measuredangle\left(\frac{\bar{\xi}_n(\boldsymbol{z})}{\bar{\xi}_n(\boldsymbol{x})}\right), \tag{26}$$

where "$\measuredangle(\cdot)$" represents the barg function defined in (21).

Solution Indeterminacy
The indeterminacy issues discussed in [33, Section 3] for the real-case estimation family also apply to estimators (26). This indeterminacy lies in the fact that $\exp(\jmath n\theta) = \exp(\jmath n(\theta + 2\pi m/n))$, for any $n, m \in \mathbb{N}$, which may lead to a non-valid separation solution. In addition, the value of $\bar{\xi}_n(\boldsymbol{x})$ (i.e., the source marginal nth-order cumulants) is not known a priori. Nevertheless, these two difficulties do not arise in all cases.

Fourth Order
At fourth-order, (24) becomes:

$$\bar{\xi}_4(\boldsymbol{z}) = (\kappa^{z}_{40} - 6\kappa^{z}_{22} + \kappa^{z}_{04}) + \jmath\jmath 4(\kappa^{z}_{31} - \kappa^{z}_{13}) = \mathrm{e}^{\jmath\jmath 4\theta}_{\alpha}(\kappa^{x}_{40} + \kappa^{x}_{04}) = \mathrm{e}^{\jmath\jmath 4\theta}_{\alpha}\gamma \,, \tag{27}$$

so that the unknown parameters can be obtained via $(4\hat{\theta}, \hat{\alpha}) = \measuredangle(\bar{\xi}_4(\boldsymbol{z})/\bar{\xi}_4(\boldsymbol{x}))$. Due to the connection with its real counterpart [30, 33], this is called the *Complex EML (CEML)* estimator. We might as well have obtained the same result by developing the 4th-order cumulants (12) directly. Effectively:

$$\begin{aligned} &\kappa^{z}_{40} - 6\kappa^{z}_{22} + \kappa^{z}_{04} = \cos(4\theta)\gamma \\ &4(\kappa^{z}_{31} - \kappa^{z}_{31}) = \mathrm{e}^{\jmath\alpha}\sin(4\theta)\gamma \,, \end{aligned} \tag{28}$$

Just like its real twin, the sks $\gamma = \bar{\xi}_4(\boldsymbol{x})$ may be obtained from the available signals as in [30]:

$$\gamma = \kappa_{40}^z + 2\kappa_{22}^z + \kappa_{04}^z = \kappa_{40}^x + \kappa_{04}^x \,. \tag{29}$$

We conclude this section with a final remark. In [6], the following relationship was found for the whitened-observation 4th-order cumulants in the real case:

$$\rho^2 - \sigma + 2 = 0, \quad \text{with} \begin{cases} \rho \triangleq \frac{\kappa_{31}^z - \kappa_{13}^z}{\kappa_{22}^z} \\ \sigma \triangleq \frac{\kappa_{40}^z + \kappa_{04}^z}{\kappa_{22}^z} \end{cases} . \tag{30}$$

Note that relating the norms of the terms at both sides of the second equality in (27), and using $|\rho|^2$ instead of ρ^2, one arrives at the complex equivalent of the above relationship.

5. Alternative Fourth-Order Estimator

5.1. The Complex AEML and a Combined Estimation Strategy

As in the real case, the CEML estimator derived from Equation (27) cannot be used for zero sks, since then $\bar{\xi}_4(\boldsymbol{x}) = 0$ (the performance degradation of this estimator around $\gamma = 0$ will be demonstrated in the experiments of Section 6). To overcome this deficiency, we resort to the complex version of the estimator put forward in [33, Section 5]. In the complex case, and by virtue of relationships (12), the associated cumulant combination develops into:

$$\bar{\xi}_4'(z) = (\kappa_{40}^z - \kappa_{04}^z) + 2\jmath\,(\kappa_{31}^z + \kappa_{13}^z) = \mathrm{e}_\alpha^{\jmath 2\theta}\eta \,, \tag{31}$$

where, $\eta = \kappa_{40}^x - \kappa_{04}^x$ represents the source kurtosis difference (skd), whose actual sign is unimportant for the estimation of the true parameters [due to equivalence class (8) and property (20d)]. Then, $(2\hat{\theta}, \hat{\alpha}) = \measuredangle \bar{\xi}_4'(z)$. For the sake of consistency in the nomenclature, we name this the *Complex AEML (CAEML)* estimator.

The same problem as in the real case about when to use (27) or (31) naturally arises at this point. In a bid to shed some light on this issue, experiments along the lines of those described in [33, Section 5.2] were carried out with the complex versions. This time, 4-QAM signals were used as sources, with independent real and imaginary parts composed of respective real-valued PRBSs with the same symbol probability. In these conditions, the (normalized) kurtosis of the resultant 4-QAM signal is $\kappa_4^x = \kappa_{4(\mathrm{PRBS})}^x/2$, so that any kurtosis value equal or greater than –1 can be obtained by suitably varying the PRBS symbol probability [28, 29]. At each separation, the interference-to-signal ratio (ISR) [31, 33] was used as a performance index:

$$\mathrm{ISR} = \mathop{\mathrm{E}}_{i \neq j} \left\{ \frac{|(\widehat{\boldsymbol{Q}}^{\mathrm{T}} \boldsymbol{Q})_{ij}|^2}{|(\widehat{\boldsymbol{Q}}^{\mathrm{T}} \boldsymbol{Q})_{ii}|^2} \right\} . \tag{32}$$

Signals were composed of $T = 5000$ samples, and the mean square value of ISR was computed over 100 Monte Carlo (MC) runs, given in dB as $\mathrm{ISR}^2(\mathrm{dB}) = 5\log_{10}(\mathrm{E}[\mathrm{ISR}^2])$. The results obtained, plotted in Figure 1, are very similar to those of [33, Section 5.2]. The alternation in best performance occurs when the skd is equal to the sks (around –1), with the CEML offering lower ISR for $|\gamma| > |\eta|$, and vice versa. Since $|\bar{\xi}_4(z)| = |\gamma|$ and $|\bar{\xi}_4'(z)| = |\eta|$ (just like for their real counterparts [33]), this leads to the conclusion that decision rule

$$|\bar{\xi}_4(z)| \underset{\text{CAEML}}{\overset{\text{CEML}}{\gtrless}} |\bar{\xi}_4'(z)| \tag{33}$$

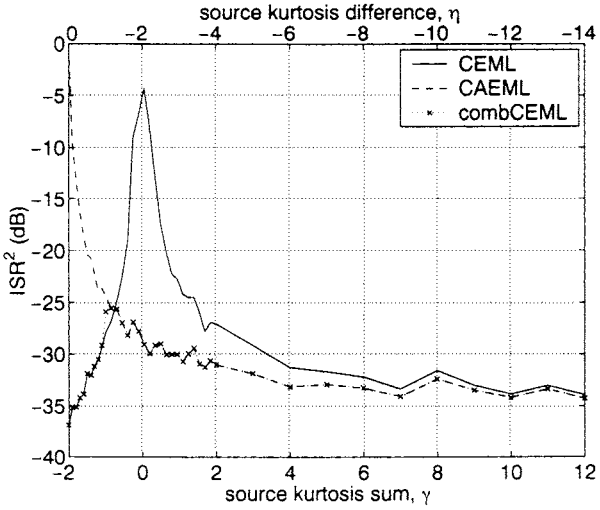

Figure 1. Performance of CEML, CAEML and combCEML vs. sks. 4-QAM sources, $\kappa_{40}^{x} = -1$, $\theta = 30°$, $\alpha = 45°$.

may as well be applied in the complex case. Although $\theta = 30°$ and $\alpha = 45°$ were used in Figure 1, this conclusion is essentially identical for all angle values (θ, α). Figure 1 also shows the results obtained under the same conditions by using the combined estimation scheme derived from the above rule, which we thus call *combined CEML (combCEML)* estimator. The performance degradation exhibited by the CEML and the CAEML around $\gamma = 0$ and $\eta = 0$, respectively, is now corrected with the combCEML.

5.2. Connections

In [7] another two-closed form estimators are proposed to solve the complex-mixture problem from the pre-whitened signals. The first one (which is also featured in [9] and [13], and we refer to as complex CF, CCF) is simply the complex extension of the real estimator developed in [6] and analyzed in [33, Section 2]. Interestingly, the second one happens to coincide with the complex alternative estimator suggested in the previous section.[1] To choose between the two, the decision rule

$$|\kappa_{22}^{z}| \underset{\text{2nd.}}{\overset{\text{1st.}}{\gtrless}} |\kappa_{31}^{z} + \kappa_{13}^{z}| \tag{34}$$

is utilized, the rationale behind it being the conditioning of the respective parameters ρ [like that in Equation (30)] of the estimators. For consistency in the nomenclature, we refer to the combined estimator derived from this rule as combined CCF (combCCF).

Herein we endow estimator (31) with a novel reformulation in terms of 4th-order cumulant bicomplex centroids, coherent with the unified notation used for the other closed-form methods considered in this paper and in [33]. This allows us: (1) to easily interrelate estimator (31) to the estimators studied in Section 4 and in [33], and (2) to obtain a practical decision rule for the combined estimation strategy developed in Section 5.1 (combCEML), which, we

[1] Note that [7, expression (13)] should actually read "$\arg\{\theta_k\} = -\arg\{\rho\} + k\pi$" when the second formula of ρ (Equation (15) therein) is employed.

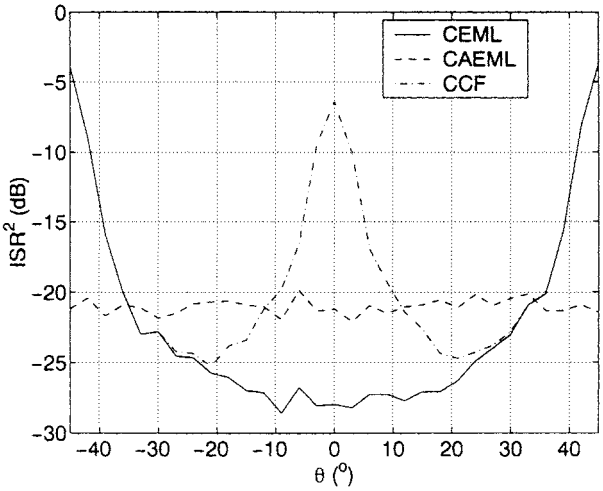

Figure 2. Mean square ISR vs. parameter θ. 16-QAM and complex Gaussian sources, $\alpha = 65°$.

anticipate, will prove more effective than the combCCF rule (34). This last claim is put to test in the next section.

6. Simulation Results

This section reports some numerical simulations that illustrate and give support to the preceding theoretical results. We also assess and compare the relevant methods in both noiseless and noisy environments. As in Section 5.1 in the experiments that follow, unless stated otherwise, all signals are composed of 5000 samples and MC iterations are run over 100 independent mixture realizations. At each MC iteration, identical signal realizations are fed into all methods considered. Performance measure ISR^2(dB) (see Section 5.1) is obtained by averaging the results over all iterations, and is the value represented at each point in the plots.

Variation with Angular Parameters
We first evaluate estimators CEML (27), CAEML (31), and CCF [7]. We are primarily concerned with their behaviour as a function of angular parameters θ and α. Figure 2 plots the results for varying θ, with 16-QAM and complex Gaussian sources. It is seen how both CCF and CEML performance depends on θ, whereas CAEML performance is independent of θ. Nevertheless, the performance of these methods is independent of parameter α, as illustrated by Figure 3.

Comparison in Noiseless Environments
In the second place, the combined estimation strategies based on decision rules (33) and (34) are assessed and compared to other methods. The other methods considered are SOK, SOK′ and JADE. Recall that the SOK is the closed-form solution given in [10] to the maximization of a 4th-order contrast function of [19]. It was shown in [33] that such solution corresponds to the EML when instead of the equal sign of source kurtosis the sign of source kurtosis sum is used. In this manner, the applicability of the contrast function was expanded, since the need for a prior knowledge of the signs of source kurtosis and for these signs to be equal is spared. Accordingly, SOK′ corresponds to solution SOK, but using in the associated algorithm

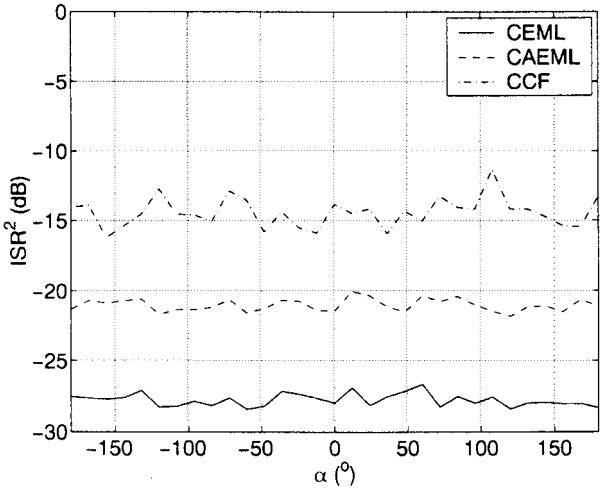

Figure 3. Mean square ISR vs. parameter α. 16-QAM and complex Gaussian sources, $\theta = 5°$.

the sign of source kurtosis sum as calculated from the whitened data by (29). On the other hand, the well-known JADE (*joint approximate diagonalization of eigenmatrices*) method is based on the optimization of another 4th-order contrast function, which can be efficiently carried out through the diagonalization of certain set of cumulant-tensor matrix slices, so-called *eigenmatrices* [4].[2]

In this comparison experiment, different sks are simulated by means of 4-QAM signals of appropriate symbol probability (as commented in Section 5.1). In a bid to smoothen the result curves, now 200 MC iterations are run at each sks point. For SOK, positive source kurtosis is assumed. Figure 4 summarizes the results. Note, first, the close performance trends between the JADE and the combCEML. On the other hand, decision rule (34) does not seem to be effective, since the combCCF performance worsens as the kurtosis of the sources tend to be similar. Results for CEML and SOK′ are exactly identical besides the region near $\gamma = 0$, around which the former improves the latter. This suggests that the conclusion drawn in [33, Section 4.3] regarding the relationship between the CEML and the SOK might perhaps be extended to the complex case as well, even though the complex SOK solution makes use of a whitened-observation 4th-order cross-cumulant which is not regarded by the CEML. However, further experiments (Figure 5) confirm that, as was to be expected from the CEML performance variation with θ evidenced by Figure 2, this similarity decreases for higher values of θ,[3] although the performances of both methods remain extremely near. Figure 5 also shows that the performance of the combCCF gets closer to that of the combCEML for higher θ.

[2] The MATLAB function implementing this method was downloaded from http://www-sig.enst.fr/~cardoso/guidesepsou.html. The pre-whitening part was skipped, since only unitary mixtures were considered in these simulations.

[3] For "high θ" is understood values of θ around $(2m + 1)\pi/4$, $m \in \mathbb{N}$, since the equivalent class of valid solutions (8) are $\frac{\pi}{2}$-periodic in θ.

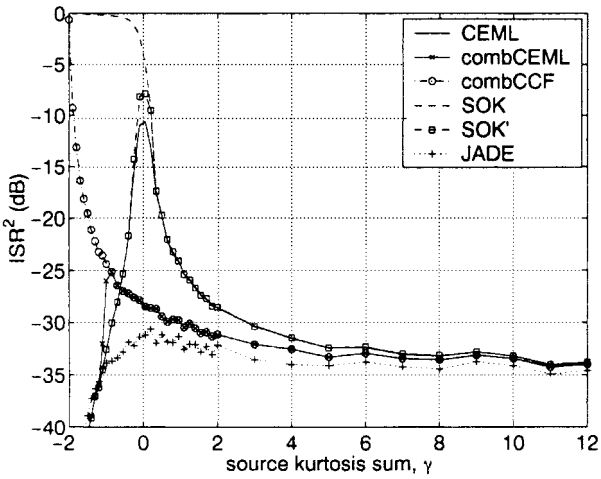

Figure 4. Mean square ISR vs. sks. 4-QAM sources, $\kappa_{40}^{x} = -1$, $\theta = 5°$, $\alpha = 65°$.

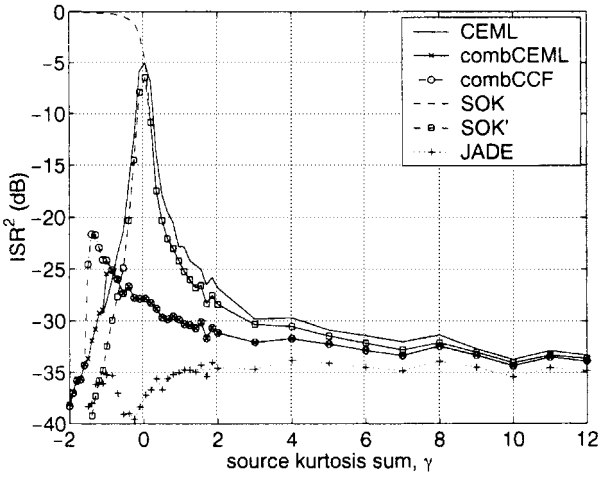

Figure 5. Mean square ISR vs. sks. 4-QAM sources, $\kappa_{40}^{x} = -1$, $\theta = 30°$, $\alpha = 65°$.

Comparison in Noisy Environments

Finally, we assess the CEML and JADE in noisy environments. Now, three sources and sensors are employed, together with the arbitrary non-unitary mixture:

$$\boldsymbol{M} = \begin{bmatrix} 1 & -1 & 1 \\ 2 & 3 & 4 \\ -2 & 1 & 3 \end{bmatrix}, \tag{35}$$

whose choice is motivated by having also been used in the real-case experiments of [32, Section 4]. Pre-whitening is carried out, for both methods, via the SVD [8, 31]. In order the extend the CEML to more than two signals, the pairwise notion originally proposed in [8] utilized. After pre-whitening, signals are processed in a two-by-two fashion, applying the suitable estimators to each signal pair in turn. The sweep over the $q(q-1)/2$ signal pairs is repeated around $(1+\sqrt{q})$ times, value which coincides with that suggested for the method of [8]. The signal-to-noise ratio (SNR) is defined sensor-wise, as the power due to the

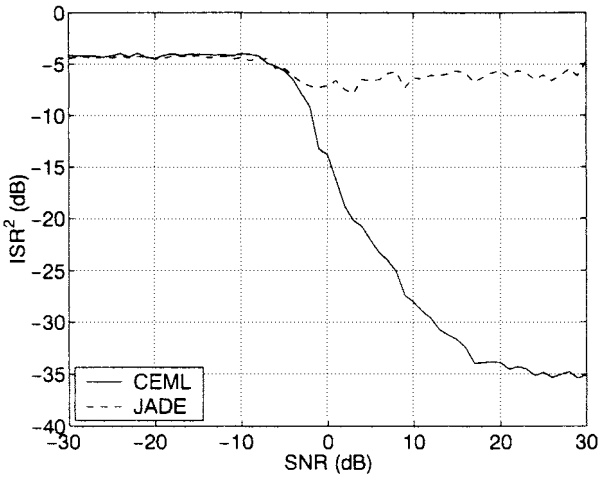

Figure 6. Mean square ISR vs. SNR, for 3 uniform-phase constant-modulus sources and 3 sensors corrupted by additive complex Gaussian noise.

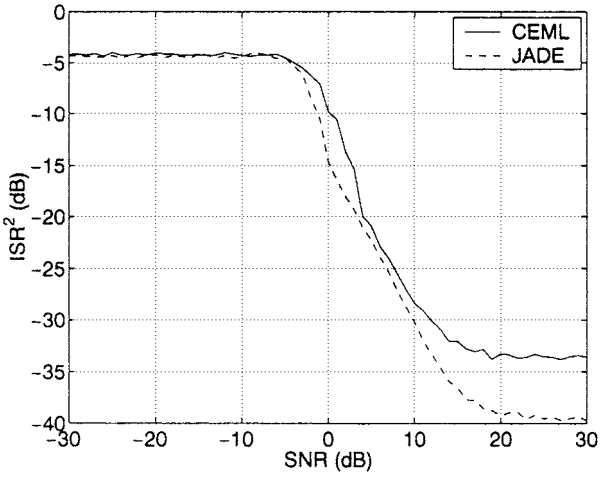

Figure 7. Mean square ISR vs. SNR, for 3 sources (2 uniform-phase constant-modulus and 1 complex-Gaussian) and 3 sensors corrupted by additive complex Gaussian noise.

sources over the power due to the noise, and chosen to be the same at all sensors. Again, we process 5000-sample signal blocks over 100 MC runs at each SNR value, ranging from –30 dB to 30 dB in 1-dB steps. Figure 6 shows the performance results for independent constant-modulus (with uniformly distributed phase in $[-\pi, \pi]$) sources in additive complex Gaussian noise. As a first conclusion, the CEML extension to more than two signals works successfully. On the other hand, remark the anomalous trend exhibited by JADE in this situation, whereas the CEML improves as the noise power decreases (high SNR), just as it is reasonable to expect. To obtain the results in Figure 7, one of the sources is changed to a complex Gaussian distribution. Now the performance of JADE improves over CEML in the positive SNR range. The reason for JADE's pathological behaviour in the previous experiment is unclear, but it seems to be observed when all sources have the aforementioned particular distribution. Similar unexpected performance was reported in [32] for the method of [8] when Toeplitz-circulant mixtures were processed under certain source and noise distribution combinations.

7. Conclusions and Outlook

In flat-fading propagation conditions, joint MUI cancellation in CDMA communication systems develops into a problem of BSS in complex-valued instantaneous linear mixtures. In the present work we have defined the bicomplex numbers, forming an isomorphic set to the group of transformations relevant to the BSS problem after pre-whitening. This algebraic formalism has permitted an elegant extension to the complex-mixture case of a number of closed-form estimation ideas originally derived in real scenarios, including the concepts of scatter diagram and centroid. The extended centroids appear as specific bicomplex linear combinations of the whitened-vector cumulants which are able to retain the information contained in the unitary mixing transformation, giving rise to compact closed-form expressions for the estimation of the pertinent parameters. Consequently, a unified formulation of the real and the complex problems within the framework of their analytical solutions has been devised.

Paths for the continuation of this investigation include the asymptotic performance analysis of the complex estimators studied in this paper, which could possibly be accomplished along the lines of the asymptotic analysis [30, 33] of their real counterparts. This analysis would explain, for example, the dependency on θ of the CEML method, which does not occur for its real equivalent [33]. Also, the theoretical study of the noise impact on the estimators' performance remains an interesting open subject. Finally, only a few properties of the new class of numbers presented in this contribution have been utilized herein; however, it is envisaged that the full potential of the bicomplex formalism may be employed in further research to generate new results on BSS, or even on problems in other fields, hence opening exciting new research directions.

References

1. P.-O. Amblard, M. Gaeta and J.-L. Lacoume, "Statistics for Complex Variables and Signals – Part I: Variables", *Signal Processing*, Vol. 53, pp. 1–13, 1996.
2. J.F. Cardoso, "On the Performance of Orthogonal Source Separation Algorithms", in *Proceedings EUSIPCO*, Edingburgh, U.K., 1994, pp. 776–779.
3. J.F. Cardoso, "The Invariant Approach to Source Separation", in *Proceedings NOLTA*, 1995, pp. 55–60.
4. J.-F. Cardoso and A. Souloumiac, "Blind Beamforming for Non-Gaussian Signals", *IEE Proceedings-F*, Vol. 140, No. 6, pp. 362–370, 1993.
5. R.M. Clemente and J.I. Acha, "Blind Separation of Sources Using a New Polynomial Equation", *IEE Electronics Letters*, Vol. 33, No. 3, pp. 176–177, 1997.
6. P. Comon, "Separation of Stochastic Processes", in *Proceedings Workshop on Higher-Order Spectral Analysis*, Vail, CO, 1989, pp. 174–179.
7. P. Comon, "Higher-Order Separation, Application to Detection and Localization", in *Proceedings EUSIPCO*, Barcelona, Spain, 1990, pp. 277–280.
8. P. Comon, "Independent Component Analysis, A New Concept?", *Signal Processing*, Vol. 36, No. 3, pp. 287–314.
9. P. Comon and P. Chevalier, "Blind Source Separation: Models, Concepts, Algorithms and Performance", in S.S. Haykin (ed.), *Unsupervised Adaptive Filtering, Vol. I: Blind Source Separation*, Wiley Series in Adaptive and Learning Systems for Communications, Signal Processing and Control, John Wiley & Sons: New York, 2000.
10. P. Comon and E. Moreau, "Improved Contrast Dedicated to Blind Separation in Communications", in *Proceedings ICASSP*, Munich, Germany, 1997, pp. 3453–3456.
11. J.A. Gallian, *Contemporary Abstract Algebra*, Houghton Mifflin Company: Boston, MA, fourth edition, 1998.
12. F. Harroy and J.-L. Lacoume, "Maximum Likelihood Estimators and Cramer–Rao Bounds in Source Separation", *Signal Processing*, Vol. 55, pp. 167–177, 1996.

13. J.-L. Lacoume, P.-O. Amblard and P. Comon, *Statistiques d'Ordre Supérieur pour le Traitement du Signal*, Collection Sciences de l'Ingénieur, Masson: Paris, 1997.
14. J.-L. Lacoume, F. Glangeaud and J. Mars, "Blind Separation of Polarized Waves", in *Proceedings EUSIPCO*, Rhodes, Greece, 1998, pp. 1629–1632.
15. L.D. Lathauwer, D. Callaerts, B.D. Moor and J. Vandewalle, "Fetal Electrocardiogram Extraction by Source Subspace Separation", in *Proceedings IEEE/ATHOS Signal Processing Conference on Higher-Order Statistics*, Girona, Spain, 1995, pp. 134–138.
16. S. Makeig, A.J.Bell, T.-P. Jung and T.J. Sejnowski, "Independent Component Analysis of Electroencephalographic Data", *Advances in Neural Information Processing Systems*, Vol. 8, pp. 145–151, 1996.
17. A. Mansour and C. Jutten, "A Direct Solution for Blind Separation of Sources", *IEEE Transactions on Signal Processing*, Vol. 44, No. 3, pp. 746–748, 1996.
18. P. McCullagh, *Tensor Methods in Statistics*, Monographs on Statistics and Applied Probability, Chapman and Hall: London.
19. E. Moreau, "Criteria for Complex Source Separation", in *Proceedings EUSIPCO*, Trieste, Italy, 1996, pp. 931–934, 1996.
20. T. Ojanperä and R. Prasad, *Wideband CDMA for Third Generation Mobile Communications*, Artech House: Boston, MA, 1998.
21. J.G. Proakis, *Digital Communications*, McGraw-Hill: New York, third edition, 1995.
22. J.J. Rieta, V. Zarzoso, J. Millet-Roig, R. García-Civera and R. Ruiz-Granell, "Atrial Activity Extraction Based on Blind Source Separation as an Alternative to QRST Cancellation for Atrial Fibrillation Analysis", in *Computers in Cardiology*, Boston, MA, pp. 67–72, 2000.
23. A. Stuart and J.K. Ord, *Kendall's Advanced Theory of Statistics, Vol. I*, Edward Arnold: London, sixth edition, 1994.
24. N. Thirion, J. Mars and J.-L. Boelle, "Separation of Seismic Signals: A New Concept Based on a Blind Algorithm", in *Proceedings EUSIPCO*, Trieste, Italy, 1996, pp. 85–88.
25. K. Torkkola, "Blind Separation for Audio Signals – Are We There Yet?", in *Proceedings 1st International Workshop on Independent Component Analysis and Signal Separation*, Aussois, France, 1999, pp. 239–244.
26. M.K. Tsatsanis and D. Slock, "Multi-User Communications/Multi-User Detection", in G. Giannakis (ed.), *IEEE Signal Processing Magazine*, "Highlights of Signal Processing for Communications", pp. 38–42, 1999.
27. S. Verdú, *Multiuser Detection*, Cambridge University Press: Cambridge, U.K., 1998.
28. V. Zarzoso, "Closed-Form Higher-Order Estimators for Blind Separation of Independent Source Signals in Instantaneous Linear Mixtures", Ph.D. Thesis, The University of Liverpool, U.K., 1999.
29. V. Zarzoso and A.K. Nandi, "Modelling Signals of Arbitrary Kurtosis for Testing BSS Methods", *IEE Electronics Letters*, Vol. 34, No. 1, pp. 29–30, 1998. (Errata: Vol. 34, No. 7, Apr. 2, 1998, p. 703.)
30. V. Zarzoso and A.K. Nandi, "Blind Separation of Independent Sources for Virtually Any Source Probability Density Function", *IEEE Transactions on Signal Processing*, Vol. 47, No. 9, pp. 2419–2432, 1999a.
31. V. Zarzoso and A.K. Nandi, "Blind Source Separation", in A.K. Nandi (ed.), *Blind Estimation Using Higher-Order Statistics*, Kluwer Academic Publishers: Boston, MA, pp. 167–252, 1999b.
32. V. Zarzoso and A.K. Nandi, "Blind Source Separation Without Optimization Criteria"", in *Proceedings ICASSP*, Vol. III, Phoenix, AZ, 1999c, pp. 1453–1456.
33. V. Zarzoso and A.K. Nandi, "Closed-Form Estimators for Blind Separation of Sources – Part I: Real Mixtures", *Wireless Personal Communications*, Vol. 21, No. 2, pp. 5–28, 2002.

Appendix. Proof of Theorem 11

The steps of the proof are just like those in [33, Theorem 1], but now we have to take into account the complex conjugations in the definition of the cumulants [Equation (9)]. Two cases must be distinguished. If n is even:

$$\kappa^z_{n-r,r} = \sum_{i_1 \ldots i_n} \underbrace{q^*_{1i_1} q_{1i_2} q^*_{1i_3} \cdot \ldots \cdot}_{n-r} \underbrace{q_{2i_{n-2}} q^*_{2i_{n-1}} q_{2i_n}}_{r} \mathrm{Cum}^x_{i_1 \ldots i_n} , \tag{36}$$

where $q_{ij} = (\boldsymbol{Q})_{ij}$. Taking into account the source independence and that $q_{11} = q_{22} = \cos\theta$, $q_{21} = -q_{12}^* = \mathrm{e}^{j\alpha}\sin\theta$, the above equation develops into:

$$\kappa^z_{n-r,r} = (\cos\theta)^{n-r}\sin^r\theta \mathrm{e}^{j\alpha(r \bmod 2)}\kappa^x_{n0} + (-\sin\theta)^{n-r}\cos^r\theta \mathrm{e}^{j\alpha((r-n) \bmod 2)}\kappa^x_{0n}\,. \tag{37}$$

Since $\jmath^r = \jmath^n\jmath^{-(n-r)} = \jmath^n(-\jmath)^{n-r}$, expression (23) becomes:

$$\begin{aligned}\bar{\xi}_n(\boldsymbol{z}) &= \sum_{r=0}^{n}\binom{n}{r}\jmath^r[(\cos\theta)^{n-r}\sin^r\theta \mathrm{e}^{j\alpha(r \bmod 2)}\kappa^x_{n0} \\ &\quad + (-\sin\theta)^{n-r}\cos^r\theta \mathrm{e}^{j\alpha((n-r) \bmod 2)}\kappa^x_{0n}] \\ &= \sum_{r=0}^{n}\binom{n}{r}(\cos\theta)^{n-r}(\jmath\sin\theta)^r \mathrm{e}^{j\alpha(r \bmod 2)}\,\kappa^x_{n0} \\ &\quad + \jmath^n\sum_{r=0}^{n}\binom{n}{r}(\jmath\sin\theta)^{n-r}\cos^r\theta \mathrm{e}^{j\alpha((n-r) \bmod 2)}\,\kappa^x_{0n}.\end{aligned} \tag{38}$$

Now, the breal part of the first summatory is

$$\binom{n}{0}\cos^n\theta - \binom{n}{2}(\cos\theta)^{n-2}\sin^2\theta + \cdots = \cos(n\theta)\,, \tag{39}$$

whereas the bimaginary part reads

$$\left[\binom{n}{1}(\cos\theta)^{n-1}\sin\theta - \binom{n}{3}(\cos\theta)^{n-3}\sin^3\theta + \cdots\right]\mathrm{e}^{j\alpha} = \mathrm{e}^{j\alpha}\sin(n\theta)\,. \tag{40}$$

The second sum produces exactly the same results. Since $\jmath^n$ is real for n even and thus it commutes with bicomplex quantities, then:

$$\bar{\xi}_n(\boldsymbol{z}) = (\cos(n\theta) + \jmath\mathrm{e}^{j\alpha}\sin(n\theta))(\kappa^x_{n0} + \jmath^n\kappa^x_{0n}) = \mathrm{e}^{\jmath n\theta}_{\alpha}(\kappa^x_{n0} + \jmath^n\kappa^x_{0n})\,. \tag{41}$$

The first half of the theorem is then proven, since $\bar{\xi}_n(\boldsymbol{x}) = \kappa^x_{n0} + \jmath^n\kappa^x_{0n}$. For n odd, however:

$$\kappa^z_{n-r,r} = \sum_{i_1\ldots i_n}\underbrace{q^*_{1i_1}q_{1i_2}q^*_{1i_3}\cdots}_{n-r}\underbrace{\cdots q^*_{2i_{n-2}}q_{2i_{n-1}}q^*_{2i_n}}_{r}\mathrm{Cum}^x_{i_1\ldots i_n}\,, \tag{42}$$

which turns into

$$\kappa^z_{n-r,r} = (\cos\theta)^{n-r}\sin^r\theta \mathrm{e}^{-j\alpha(r \bmod 2)}\kappa^x_{n0} + (-\sin\theta)^{n-r}\cos^r\theta \mathrm{e}^{j\alpha((n-r) \bmod 2)}\kappa^x_{0n}\,. \tag{43}$$

So now the bimaginary part of the first sum becomes $\mathrm{e}^{-j\alpha}\sin(n\theta)$, whereas the rest of the terms remain just as before. Hence

$$\begin{aligned}\bar{\xi}_n(\boldsymbol{z}) &= (\cos(n\theta) + \jmath\mathrm{e}^{j\alpha}\sin(n\theta))\kappa^x_{n0} + \jmath^n(\cos(n\theta) + \jmath\mathrm{e}^{j\alpha}\sin(n\theta))\kappa^x_{0n} \\ &= \mathrm{e}^{\jmath n\theta}_{-\alpha}\kappa^x_{n0} + \jmath^n\mathrm{e}^{\jmath n\theta}_{\alpha}\kappa^x_{0n}\,.\end{aligned}$$

But $\jmath\mathrm{e}^{\jmath n\theta}_{\alpha} = \mathrm{e}^{\jmath n\theta}_{-\alpha}\jmath$, and then $\bar{\xi}_n(\boldsymbol{z}) = \mathrm{e}^{\jmath n\theta}_{-\alpha}(\kappa^x_{n0} + \jmath^n\kappa^x_{0n})$ for n odd. Therefore $\forall n : \bar{\xi}_n(\boldsymbol{z}) = \mathrm{e}^{\jmath n\theta}_{(-1)^n\alpha}\bar{\xi}(\boldsymbol{x})$. □

Vicente Zarzoso was born in Valencia, Spain, on September 12, 1973. He attended the Universidad Politécnica de Valencia for the first four years of his degree, and the University of Strathclyde, Glasgow, U.K., on an Erasmus exchange programme for the final year his degree. In July 1996, he received the M.Eng. degree with the highest distinction (Premio Extraordinario de Terminación de Estudios) in telecommunications engineering from the Universidad Politécnica de Valencia. He was awarded a scholarship by the University of Strathclyde to study in the Signal Processing Division of the Department of Electronic and Electrical Engineering towards his Ph.D. degree, the first year of which was also partly funded by a grant from the Defence Evaluation and Research Agency (DERA) of the U.K. He received the Ph.D. degree from the Department of Electrical Engineering and Electronics. The University of Liverpool, Liverpool, U.K. in October 1999.

Since March 1999, he has been with the Signal Processing and Communications Group, Department of Electrical Engineering and Electronics, The University of Liverpool, Liverpool, U.K. He holds a Post-doctoral Research Fellowship awarded by the Royal Academy of Engineering, Westminster, London, U.K. His research interests include blind signal separation, higher-order statistics, statistical signal and array processing, and their application to communications and biomedical problems.

Asoke K. Nandi received the degree of Ph.D. from the University of Cambridge (Trinity College), U.K., in 1979. He held a scholarship at Trinity College during his doctoral studies at the Cavendish Laboratory, Cambridge. Since then he held several research positions: associateship in Rutherford Appleton Laboratory, Oxfordshire, U.K., and in the European Organization

for Nuclear Research (CERN), Geneva, Switzerland, as well as Advanced Fellowship in the Department of Physics, Queen Mary College, London, U.K., and in the Department of Nuclear Physics, University of Oxford, U.K. In 1987, he joined the Imperial College, London, U.K., as the Solartron Lecturer in the Signal Processing Section of the Electrical Engineering Department. In 1991, he joined the Signal Processing Division of the Electronic and Electrical Engineering Department in the University of Strathclyde, Glasgow, U.K., as a Senior Lecturer; subsequently, he was appointed a Reader in 1995 and a Professor in 1998. In March 1999, he moved to the University of Liverpool, U.K., to take up the appointment to the David Jardine Chair of Electrical Engineering in the Department of Electrical Engineering and Electronics.

In 1983 he was part of the UAI team at CERN that discovered the three fundamental particles known as W^+, W^- and Z^0 providing the evidence for the unification of the electromagnetic and weak forces, which was recognized by the Nobel committee for Physics in 1984. Currently he is the head of the signal processing and communications research group, which includes a number of tenured academics and a group of doctoral and post-doctoral researchers with interests in the areas of nonlinear systems, non-Gaussian signal processing, and communications research. With his group he has been carrying out research in machine condition monitoring, signal modelling, system identification, communication signal processing, time delay estimation, biomedical signals, underwater sonar, application of artificial neural networks, ultrasonics, blind source separation, and blind deconvolution. Professor Nandi was awarded the Mountbatten Premium, Division Award of the Electronics and Communications Division, of the Institution of Electrical Engineers of the U.K. in 1998 and the Water Arbitration Prize of the Institution of Mechanical Engineers of the U.K. in 1999.

Professor Nandi has authored or coauthored over 200 technical publications including two books – titled *Automatic Modulation Recognition of Communication Signals* (1996) and *Blind Estimation Using Higher-Order Statistics* (1999) – and over 100 journal papers. He is a Fellow of the Cambridge Philosophical Society, the Institution of Electrical Engineers, the Institute of Mathematics and its Applications, and the Institute of Physics. Also, he is a Senior Member of the Institute of Electrical and Electronic Engineers as well as a Member of the British Computer Society and the European Association for Signal Processing.